6th International Conference on Contemporary Problems of Thermal Engineering
CPOTE 2020, 20-24 September 2020, Kraków, Poland

Thermal analysis of a low voltage winding of a power transformer working with natural ester and mineral oil

A. **Santisteban[1*], J. Dorella[2], L. Garelli[2], M. Storti[2], F. Delgado[1], A. Ortiz[1]**
[1]Department of Electrical and Energy Engineering
ETSIIT, University of Cantabria
39005 Santander, Spain
e-mail: santistebana@unican.es

[2]Centro de Investigación de Métodos Computacionales
CIMEC (UNL-CONICET)
3000 Santa Fe, Argentina

Keywords: CFD, Power transformer, thermal modelling, mineral oil, natural ester

Abstract

In this work a thermal-hydraulic analysis of the low voltage winding of a power transformer working in oil natural mode will be performed. The study considers the thermal and hydraulic balance of the cooling loop to determine the mass flow and oil temperature at the inlet of the winding. Balance of the windings and radiator determine the boundary conditions of the model. The thermal model of the winding is performed using Computational Fluid Dynamics. The winding simulations are made with a 2D axisymmetric model run with the commercial code ANSYS Fluent. Several phenomena appear in the winding, due its configuration, that affects the heat transfer in local regions, reducing the local hot-spots in regions where the oil mass flow is low. The results will be compared to those obtained when the mineral oil is replaced by a natural ester. For natural ester, the same phenomena appears with lower intensity due to the lower mass flow and the higher viscosity. The results of this study predicts 5.7 degrees lower bottom-oil temperature and 48% lower mass flow rate at the winding for the natural ester compared to mineral oil. The reduction of mass flow through the winding is caused by the high viscosity of the natural ester. Also, the reduction of the mass flow leads to lower bottom-oil temperature. Regarding the winding model, mineral oil shows 7.3 degrees lower hot-spot temperature than the natural ester case.

1 Introduction

Oil-immersed power transformers are one of the most expensive and critical components of an electrical system. Despite being highly-efficient machines, a small fraction of the transferred power is lost in the form of heat (mainly in the windings), which must be removed. A heat-carrier dielectric fluid, generally

a mineral oil, is used to remove the generated heat, and simultaneously provide electrical insulation. This liquid circulates around the windings cooling them, and thus preventing hotspots that negatively affects to the transformer lifetime. The dimensions of these cooling channels depend on the dielectric fluid properties, as well as the structural and electrical requirements, [1].

One of the most extended techniques for the thermal modelling of power transformers is the Computational Fluid Dynamics (CFD). In CFD, the governing principles of both fluid flow and heat transfer are written in the form of partial differential equations that are then replaced by algebraic equations and solved at discrete elements in time and space. During the last two decades, several authors have reported the CFD technique as a relevant tool to investigate and improve the thermal performance of power transformers windings. In the first decade, the main purpose of CFD was to determine the velocity and temperature profiles of a 2-D winding immersed in a mineral oil, [2]–[7]. More recently, the improvement of computational resources has enabled the use of 3-D models to conduct numerical investigations, allowing to capture three-dimensional phenomena that are impossible to find in 2-D models, [8]–[11].

More recent studies have been carried out using both 2-D and 3-D models to better understand and characterize the thermal-hydraulic performance of the insulation systems (oil and paper) with ester-based oils, [12], [13], as well as to evaluate the cooling efficiency of several alternative liquids, [14]–[16] . Regarding the aging of the transformer insulation, several studies have determined that natural ester reduces the aging rate of the insulation paper. In these studies, accelerated aging test where performed and the degree of polymerization and tensile strength were tested when immersed in mineral oil and natural ester [13], [17]–[21].

In this work, a comparative study of the cooling of a transformer winding with mineral oil and natural ester is made. Global balance of the transformer cooling circuit is done in order to adjust the inlet conditions for the comparison.

2 Model description

In this part, the model description used for the CFD model will be introduced. Transformer geometry, materials and CFD model and mesh will be presented in this section.

2.1 Geometry

In this work, the flow behavior and temperatures inside the windings of an 8.5 MVA – 33/6.9 kV ONAN (Oil Natural Air Natural) power transformer is studied. This transformer is actually designed and produced by the manufacturer Tadeo Czerweny S.A. As can be seen from Table 1, the low voltage winding consist of 50 discs and the high voltage winding consists of 58 discs. Low voltage winding discs are 66 mm wide and 11.5 mm high whereas high voltage winding discs are 72 mm wide and 8.6 mm high. The inner and axial ducts are 6 mm width, except for the outer axial duct in the low voltage winding which is 7 mm width. The spacers of the low voltage winding are 4.5 mm high and the high voltage winding spacers are 5 mm high, leading to a total winding height of 804 mm and 792 mm for low and high voltage windings, respectively.

With this data, CFD modelling of the low voltage winding of the transformer will be performed. 2D axisymmetric models will be used for the CFD analysis.

Table 1: Geometrical information of the transformer winding

	Low voltage winding	High voltage winding
Type	Disc	Disc
Number of discs	50	58
Internal diameter	417 mm	585 mm
Radial disc dimension	66 mm	72 mm
Disc height	11.5 mm	8.6 mm
Winding height	804 mm	792 mm

Inner duct width	6 mm	6 mm
Outer duct width	7 mm	6 mm

2.2 Materials

In this section the properties of the materials that form the insulation system of the winding are described. The insulation materials that are included in the CFD model are the insulating fluid and the insulation paper. Other insulating materials, such as cardboard, are not considered in the model. Due to their low thermal conductivity are considered as adiabatic walls.

2.2.1 Dielectric fluid

Two different kinds of dielectric fluid are considered in this study. Mineral oils and natural esters will be considered for the cooling of the transformer windings. For the insulating fluids, the temperature dependent properties are known and collected in Table 2. These equations are valid in the range of temperature inside the transformer winding (up to 100degC).

Table 2: Temperature dependent properties of dielectric fluids

	Mineral oil	Natural ester
Density (kg/m^3)	$1098.72 - 0.712 \cdot T$	$1109.2 - 0.653 \cdot T$
Specific heat (J/kg·K)	$807.163 + 3.58 \cdot T$	$1273.15 + 1.952 \cdot T$
Conductivity (W/m^2·K)	$0.1509 - 7.101e-5 \cdot T$	$0.1317 + 4.142e-4 \cdot T - -8.86e-7 \cdot T^2$
Viscosity (Pa·s)	$0.08467 - 4e-4 \cdot T + +5e-7 \cdot T^2$	$7.99 - 6.63e-2 \cdot T + +1.84e-4 \cdot T^2 - 1.71e-7 \cdot T^3$

Since both fluids show a linear dependence with the temperature for the density, the Boussinessq approach will be used. By using this approach, the computational time will be reduced. Although the temperature rise will be higher than the recommended of 10K, the linear dependence on temperature of the density still stands. In [1] considered both kinds of model for a part of a transformer winding without significant variation.

2.2.2 Equivalent thermal conductivity

The winding discs are normally formed by a set of copper conductors wrapped with insulation paper. This structure has to be modelled for a detailed analysis of the temperature distribution on the discs, increasing the complexity of the geometry and the computational cost. In order to simplify the solid domain for CFD simulations, equivalent values for thermal conductivity of the discs are calculated in this section. The goal of this process is to avoid modelling the conductor and insulation system in detail, leading to a simpler design building the discs as unique material with the equivalent thermal conductivity of the real system. The impact of this approach over the average and maximum disc temperatures is not important.

The low voltage discs are made of 2.2x11 mm rectangular cross section conductors and the high voltage discs are made of 2x8.1 mm rectangular cross section conductors. Both conductors are wrapped with insulation paper with a thickness of 0.25 mm. Since the axial and radial dimensions of the disc are different, the equivalent material will have an orthotropic thermal conductivity in cylindrical coordinates. Assuming thermal conductivities of 400 and 0.19 W/m·K for conductor and paper, respectively, the equivalent thermal conductivities of the discs are presented in Table 3.

Table 3: Temperature dependent properties of dielectric fluids

	Low voltage winding	High voltage winding
k_{rad}	1.024 W/m·K	0.948 W/m·K
k_{ax}	4.325 W/m·K	3.243 W/m·K

Using these values, the disc can be model as a unique block, which makes easier the geometry building and the meshing step.

2.3 Transformer balance

The next step is trying to estimate the inlet mass flow through the windings as well as the inlet temperature. To perform these calculations, some simplifications have been made:

- The pressure drop on the windings is generated mainly by friction through axial ducts, since radial flow is very low compared to axial flow.
- The pressure drop on the radiator is assumed to be equal to the pressure drop in one panel, with a uniform distribution of the mass flow in the radiator panels.
- The top oil temperature at the core is the same as the top oil temperature of the transformer.
- The power dissipated by the radiators is the same for all radiator installed in the transformer.
- The center point of the radiator is located 450 mm above the center point of the windings (this value has been taken from Rios *et al.* 2017 [2])
- Fluid properties are considered constant (Boussinesq approach) at a reference temperature, which is the bottom oil temperature.
- ~~The calculations are made for a 2D axisymmetric model (areas and hydraulic diameter calculations stands for 2D geometries).~~

Based on the geometrical data available and the assumptions previously mentioned the mass flow inlet and bottom oil temperature could be calculated by applying the balance equations to the windings and radiator. The calculation process is also explained in [3].

2.3.1 Hydraulic balance

Taking into account that the transformer has an ONAN cooling system, the unique source for the driving pressure is the thermal driving pressure, which is expressed in eq.(1)

$$p_T = \rho_{ref} \cdot g \cdot \beta \cdot \Delta T \cdot \Delta H \quad (1)$$

Where ρ_{ref} is the oil density at the reference temperature, g is the gravity acceleration, β is the thermal expansion coefficient of the oil, ΔT is the oil temperature rise and ΔH is the distance between radiator and windings center points.
This value should be equal to the total pressure drop of the cooling circuit, which is assumed that is the sum of the winding and the radiator pressure drop, leading to eq.(2)

$$p_T = \Delta p_{wind} + \Delta p_{rad} \quad (2)$$

From eq.(2), the temperature rise is unknown, as well as the mass flow through windings and radiator. The windings are assumed that are parallel circuits so the pressure drop will be the same for both high voltage and low voltage windings.

$$\Delta p_{lvw} = \Delta p_{hvw} \quad (3)$$

2.3.2 Thermal balance

From the hydraulic balance, eqs. (2) and (3) have been proposed but there are four unknowns for two equations. In order to get the same number of equations and unknowns, the thermal balance is applied to the transformer components leading to eqs.(4-8)

$$P_{core} = \dot{m}_{core} \cdot c_p \cdot \Delta T \quad (4)$$

$$P_{lvw} = \dot{m}_{lvw} \cdot c_p \cdot \Delta T_{lvw} \quad (5)$$

$$P_{hvw} = \dot{m}_{hvw} \cdot c_p \cdot \Delta T_{hvw} \quad (6)$$

$$P_{rad} = \dot{m}_{rad} \cdot c_p \cdot \Delta T \quad (7)$$

$$P_{tot} = \dot{m}_{tot} \cdot c_p \cdot \Delta T \quad (8)$$

Eqs.(4-8) introduce five unknowns that are the mass flow through core, radiator and total of the transformer and the temperature rise in low voltage and high voltage windings. Considering that the total mass flow is the sum of the low voltage winding, high voltage winding and core mass flow rates, and that the top oil temperature is related to the top oil temperature of each component, eqs.(9-10) are obtained.

$$\dot{m}_{tot} = \dot{m}_{lvw} + \dot{m}_{hvw} + \dot{m}_{core} \quad (9)$$

$$\dot{m}_{tot} \cdot c_p \cdot T_{to} = \dot{m}_{lvw} \cdot c_p \cdot T_{to-lvw} + \dot{m}_{hvw} \cdot c_p \cdot T_{to-hvw} + \dot{m}_{core} \cdot c_p \cdot T_{to} \quad (10)$$

Considering eqs.(5), (6) and (10) the temperature rise of the transformer can be expressed as eq.(11)

$$\Delta T = \frac{P_{lvw} + P_{hvw}}{(m_{lvw} + m_{hvw}) \cdot c_p} \quad (11)$$

Now, considering equations (2), (3), (7) and (11) there are four unknowns that are the temperature rise and the mass flow rate through radiator, low voltage winding and high voltage winding. However, the top oil and bottom oil temperatures are still unknown. For that, the thermal balance of the radiator is expressed in eq. (12)

$$P_{rad} = \dot{m}_{rad} \cdot c_p \cdot (T_{to} - T_a) \cdot \left(1 - e^{-\frac{k_p \cdot O \cdot L_r}{\dot{m}_{rad} \cdot c_p}}\right) \quad (12)$$

Where k_p is the global heat transfer coefficient of the radiator, the $O \cdot L_r$ product represents the surface exchange area of the radiator and T_a is the ambient temperature.

2.4 Mesh independence test

The next step of the analysis is to determine the mesh influence on the results by performing a mesh independence test. For this reasons, three different meshes has been made for the low voltage winding problems, and the results are compared in order to select the correct mesh size that has no influence on the results and leads to the shortest computation time possible.

Three different meshes of 170k, 665k and 2.6M elements have been generated for the test, with a reference mesh size of 0.4, 0.2 and 0.1 mm, respectively. Average and maximum disc temperatures and mass flow rates through radial ducts have been taken into account to determine if the influence of the mesh can be considered negligible.

For the intermediate and the coarse meshes, the deviations on the average disc temperature are below 2.26 K, with an average deviation of 0.75 K. For the maximum disc temperature, the maximum deviation observed is 2.55 K and the average deviation is 0.87 K. Regarding the intermediate and fine meshes, these deviations are maximum and average deviations in average disc temperature of 0.58 and 0.21 K. For maximum disc temperature, these deviations are 0.63 and 0.25 K. Table 4 collects the deviations observed for the test.

Table 4: Results deviation in mesh independence test

		Coarse-intermediate mesh	Intermediate-fine mesh
Average disc temperature	Average	0.75 K	0.22 K
	Maximum	2.27 K	0.58 K
Maximum disc temperature	Average	0.87 K	0.25 K
	Maximum	2.55 K	0.63 K
Mass flow rate	Average	7.87e-5 kg/s	1.73e-5 kg/s
	maximum	2.23e-4 kg/s	5.72e-5 kg/s

With this results, can be expected that the intermediate mesh is accurate enough to perform the CFD analysis. In addition, the uncertainty of the intermediate mesh has been tested using the Richardson extrapolation for the average and maximum disc temperature, using as a reference the maximum temperature rise. The maximum uncertainty of the mesh is 2.7% and the uncertainty of the hot-spot temperature, which is the most interesting point, is 1.29%.

2.5 Boundary conditions

For the proposed model, the inlet mass flow rate and temperature of the oil is calculated following the procedure previously described. Also the power losses in the winding are represented by a heat source in the winding discs. The outer walls of the winding, made of cardboard of low thermal conductivity, are considered as adiabatic. Boussinesq approach is considered for the gravity driven flow in the effect of mixed convection model. Table 5 presents the calculated values for the inlet conditions to the CFD simulations.

Table 5: Temperature dependent properties of dielectric fluids

	Mineral oil	Natural ester 01
$\dot{m}_{lvw}$	0.127 kg/s	0.0716 kg/s
$\dot{m}_{hvw}$	0.131 kg/s	0.0739 kg/s
T_{bo}	328.58 K	323.62 K
ΔT	14.3 K	26.4 K

From Table 5, mass flow rate through low voltage winding and bottom oil temperature will be considered as boundary conditions. It can be appreciated that in the case of natural ester the flow is 44% lower than the mineral oil case due to the higher viscosity of the ester. In addition, due to lower mass flow rates, the bottom oil temperature of the natural ester is 5K lower than the mineral oil.

3 Results and discussion

3.1 Mineral oil

For the mineral oil case, results shows low mass flow rate through radial channel, being this value lower than 2% of the total mass flow of the winding. The flow through radial ducts changes its directions several times along the winding. This effect leads to local heated parts in the winding. The hot spot temperature is located in the upper part due to isolation in the top disc, leading to a temperature rise in the upper discs of the winding. A hot spot temperature of 366.6 K and an average winding temperature of 351.7 K are obtained from this simulation.

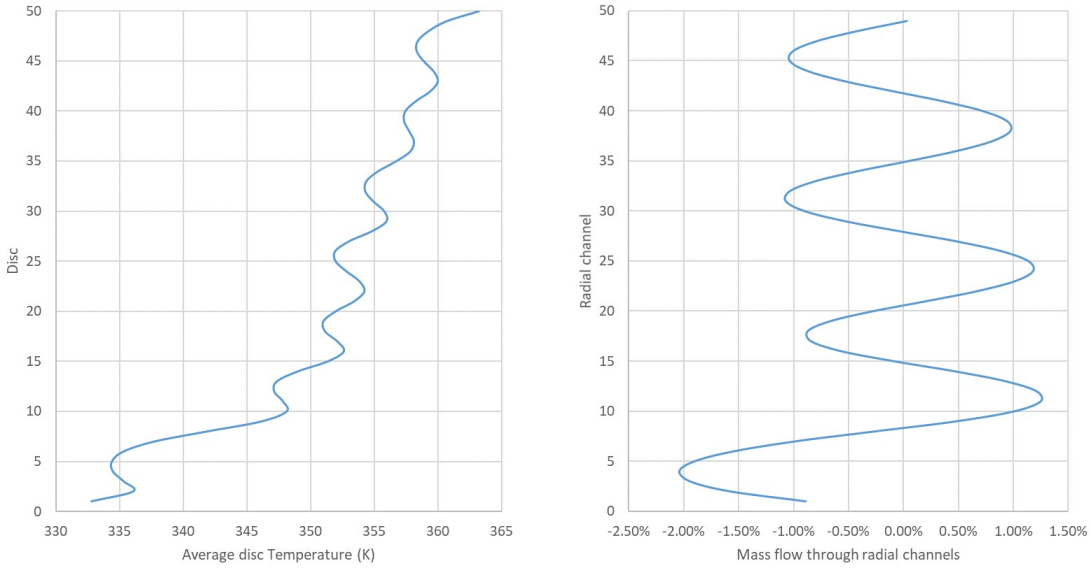

Figure 1: Temperature and mass flow rate profiles

Although the mass flow rate through radial channels is low, some intern effects appears than increase the local cooling of the discs. In this case, counterflow has been appreciated looking at the velocity vectors, creating a convective loop that increases the heat transfer coefficient of the duct. Figure 2 shows this effect in radial ducts of the transformer winding.

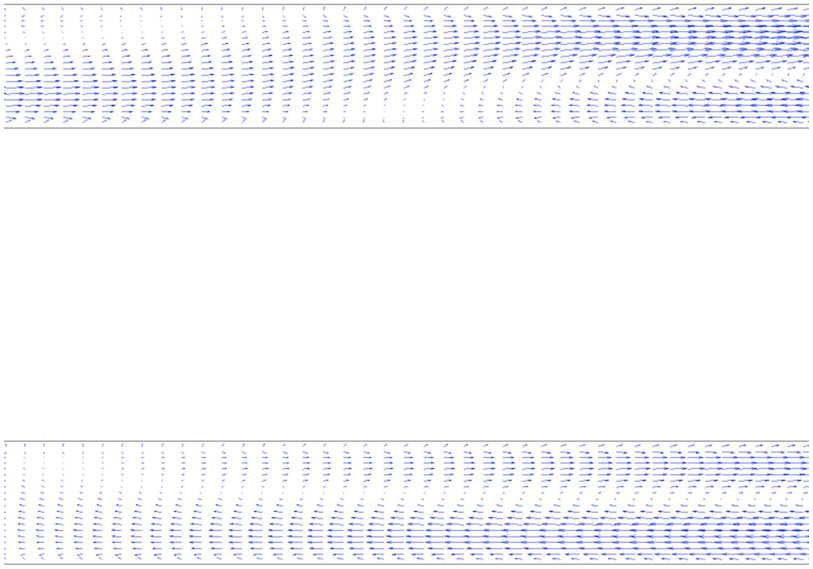

Figure 2: Velocity vectors in radial ducts

Figure 3 shows the temperature field of the winding. In the picture can be appreciated the local maximum temperatures as well as the change of direction of the mass flow rate through radial ducts.

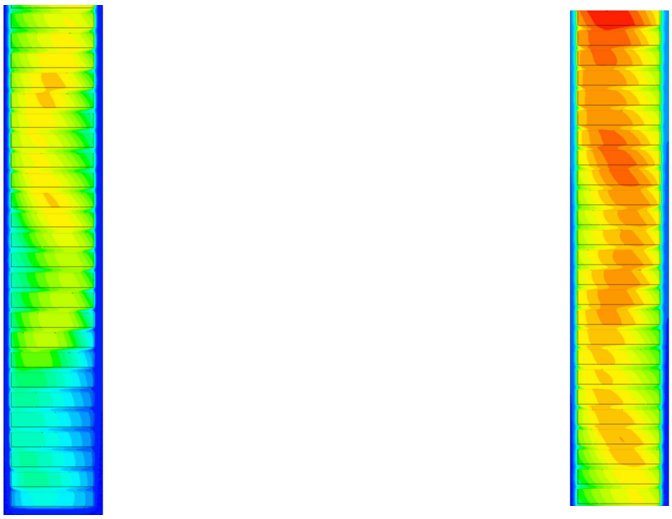

(a) *(b)*

Figure 3: Temperature field of the winding. (a) bottom part of the winding (b) top part of the winding

3.2 Natural ester

In the case of natural ester, same behavior as the mineral case is observed in the mass flow rate through radial ducts and in the average temperature profile. The change of direction of the flow rate in radial ducts leads to local maximum in the discs temperature. A hot spot temperature of 373.9 K, located on the top of the winding, and an average winding temperature of 352.4 K are obtained from this simulation.

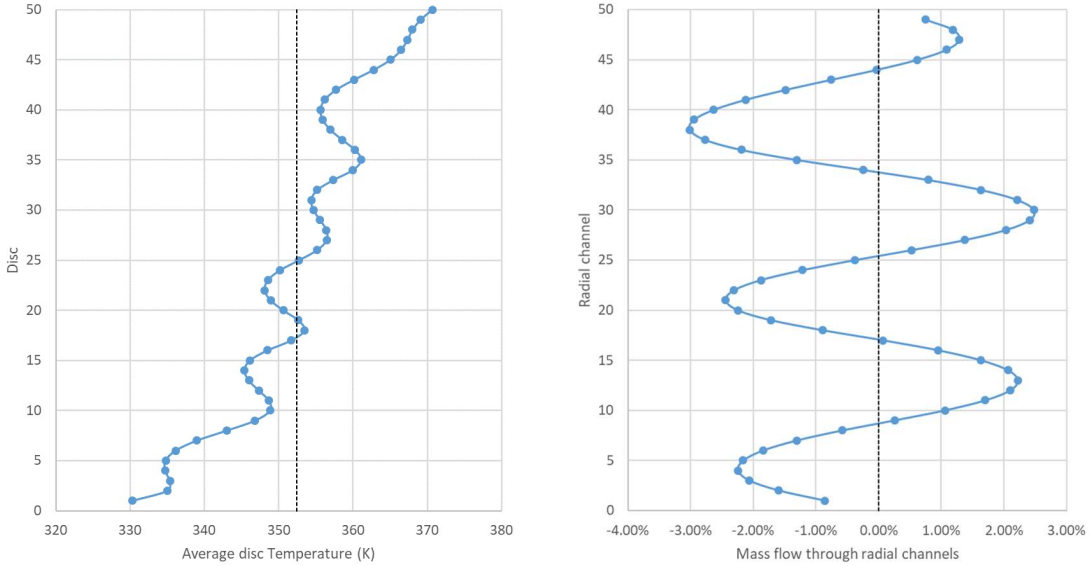

Figure 4: Temperature and mass flow distribution in the winding

As happened with the mineral oil case, convective loops appears in the radial ducts with low total mass flow rate. In this case, these flows have less influence that in the mineral oil case, due to the higher viscosity of the ester that difficult the formation of these flows.

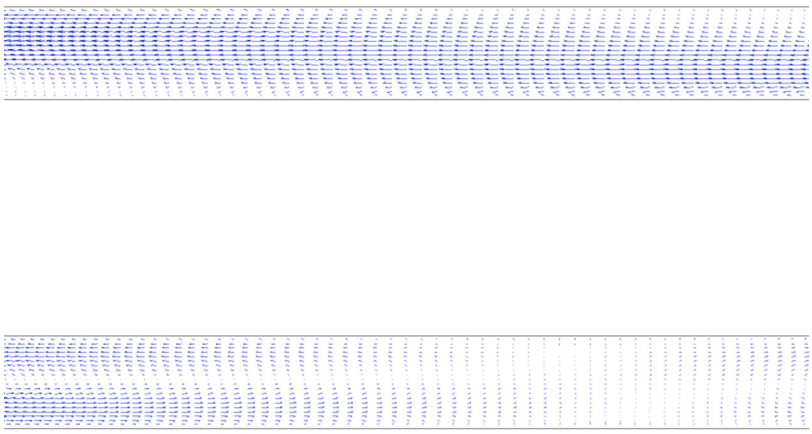

Figure 5: Velocity vectors in radial ducts

Regarding the temperature field, same effect as in mineral oil happens, where can be observed the change of direction of the mass flow rate through radial ducts.

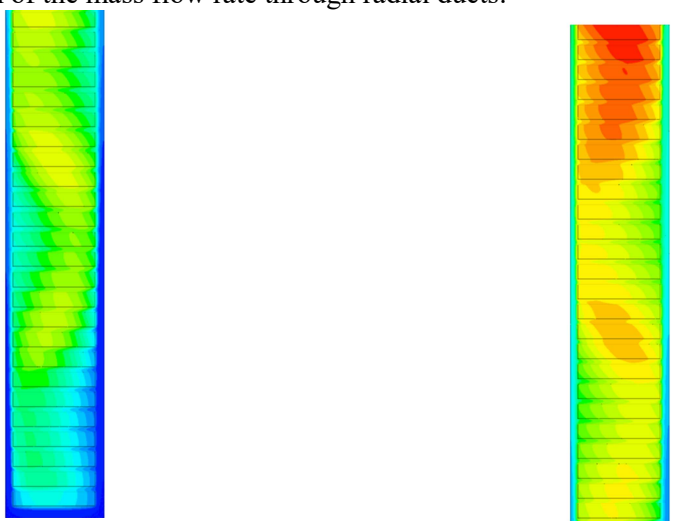

(a) *(b)*

Figure 6: Temperature field of the winding. (a) bottom part of the winding (b) top part of the winding

3.3 Discussion

In this work, two different scenarios are presented and compared. Same power transformer with two different cooling dielectric fluids that leads to different mass flow rates and temperatures at the inlet of the winding. Since the natural ester has higher viscosity, lower mass flow rate through winding is observed. In addition to lower mass flow rate, inlet temperature is lower than the case of mineral oil. This values comes from the transformer balance explained in previous sections and are taken as inlet conditions for the CFD simulations.

Regarding the CFD simulations, similar behavior of the oil flow through radial duct has been observed. Due to the buoyancy driven flow, Reynolds number is below 10, the direction of the mass flow rate in radial duct changes its direction. In addition, convective loops appear in the radial ducts where the mass flow rate is low, increasing the heat transfer coefficient and the winding cooling. These flows are more important in mineral oil, where the viscosity is low compared to natural ester.

Regarding the winding temperatures, Table 6 shows the inlet conditions and hot spot temperature and temperature rises observed in both cases. Can be appreciated that natural ester leads to lower mass flow rate, higher temperature rises and higher hot spot temperature.

Table 6: Temperature dependent properties of dielectric fluids

	Mass flow inlet	Temperature inlet	Hot spot temperature	Temperature rise
Mineral oil	0.125 kg/s	323.2K	366.6K	43.4K
Natural ester	0.065 kg/s	317.5K	373.9K	56.4K

4 Conclusions

In this work, the cooling performance of two different dielectric fluids inside a power transformer winding has been compared. Regarding the global cooling circuit, the natural ester presents lower mass flow rate through the circuit. This is due to the higher viscosity of the natural ester compared to mineral oil, in a buoyancy driven system. The reduction of mass flow rate leads to higher temperature rise and higher thermal driving force, which balance the cooling system. In addition, lower mass flow rate in radiators allows lower oil-to-ambient temperature difference to be lower than in the case of mineral oil. This effects cause that in the case of natural ester, the mass flow rate and the bottom-oil temperature is lower than the mineral oil.

In the winding it was observed that the mass flow rate through radial ducts is a small fraction of the total flow in this winding configuration. Without any elements that impose the radial flow, the fluid tends to flow through axial ducts, where the hydraulic resistance is lower. However, in the radial ducts where the mass flow is low, convective flows appears, increasing the heat transfer coefficient on this part and improving the cooling winding. This effect occurs at very low Re numbers and is related to natural convection and buoyancy.

Regarding the temperatures, natural esters shows a higher hot-spot temperature than mineral oil. This is mainly caused by the difference of the mass flow rate that enters in the winding, that is 53% of the mineral oil mass flow rate. This leads to a hot spot temperature 7.3K higher in the case of natural ester. The bottom oil to hot spot temperature rise is higher for the natural ester since the bottom oil is lower and the hot spot temperature is higher.

Nomenclature

c_p	specific heat
g	acceleration of gravity
k_{ax}	thermal conductivity in the axial direction
k_{rad}	thermal conductivity in the radial direction
k_p	global heat transfer coefficient of radiator panel
L_r	length of radiator panel
$\dot{m}_{core}$	mass flow rate through core
$\dot{m}_{hvw}$	mass flow rate through high voltage winding
$\dot{m}_{lvw}$	mass flow rate through low voltage winding
$\dot{m}_{rad}$	mass flow rate through radiator
$\dot{m}_{tot}$	total mass flow rate in the cooling circuit
O	circumference of radiator outer cross section
P_{core}	power losses in transformer core
P_{hvw}	power losses in high voltage winding
P_{lvw}	power losses in low voltage winding
P_{rad}	power dissipated by radiator
p_T	thermal driving pressure
P_{tot}	total power losses of the transformer
T	temperature
T_a	ambient temperature
T_{bo}	bottom oil temperature

T_{to}	top oil temperature
$T_{to\text{-}hvw}$	top oil temperature in high voltage winding
$T_{to\text{-}lvw}$	top oil temperature in low voltage winding
β	thermal expansion coefficient of the fluid
ΔH	height difference from radiator center point to winding center point
Δp_{hvw}	pressure drop in high voltage winding
Δp_{lvw}	pressure drop in low voltage winding
Δp_{rad}	pressure drop in radiator
Δp_{wind}	pressure drop in the winding system
ΔT	oil temperature rise in the transformer
ΔT_{hvw}	oil temperature rise in high voltage winding
ΔT_{lvw}	oil temperature rise in low voltage winding
ρ_{ref}	oil density at reference temperature

Acknowledgements

Funding: This research is under BIOTRAFO project – "Raising Knowledge and Developing Technology for the Design and Deployment of High Performance Power Transformers Immersed in Biodegradable Fluids", that has received funding from the European Union Comision's Horizon 2020 research and innovation program under the Marie Sklodowska-Curie grant agreement H2020-MSCARISE-2018- 823969; 2019-21.

The authors of this research wish to thank the Spanish Ministry of Economy for its financial support for the National Research Project: "Improvement of Insulation Systems of Transformers through Dielectric Nanofluids: Thermodynamic Characterizations and Modelling" (DPI2015-71219-C2 1-R). Also, they want to thank the Regional Government of Cantabria, more precisely the Department of Universities, Research, Environment and Social Policy, for its financial support for the Project "Fluidos Biodegradables en Transformadores Eléctricos de Potencia: Impregnación de Dieléctricos Sólidos y Modelado Térmico con THNM".

References

[1] "Electrical Insulating Oils," in *ASTM Special Technical Publication*, 1988.
[2] J. M. Mufuta and E. Van Den Bulck, "Modelling of the mixed convection in the windings of a disc-type power transformer," *Appl. Therm. Eng.*, vol. 20, no. 5, pp. 417–437, 2000.
[3] N. El Wakil, N.-C. Chereches, and J. Padet, "Numerical study of heat transfer and fluid flow in a power transformer," *Int. J. Therm. Sci.*, vol. 45, no. 6, pp. 615–626, 2006.
[4] E. Rahimpour, M. Barati, and M. Schäfer, "An investigation of parameters affecting the temperature rise in windings with zigzag cooling flow path," *Appl. Therm. Eng.*, vol. 27, no. 11–12, pp. 1923–1930, 2007.
[5] J. Smolka, O. Bíró, and A. J. Nowak, "Numerical simulation and experimental validation of coupled flow, heat transfer and electromagnetic problems in electrical transformers," *Arch. Comput. Methods Eng.*, vol. 16, no. 3, pp. 319–355, 2009.
[6] F. Torriano, M. Chaaban, and P. Picher, "Numerical study of parameters affecting the temperature distribution in a disc-type transformer winding," *Appl. Therm. Eng.*, vol. 30, no. 14–15, pp. 2034–2044, 2010.
[7] A. Skillen, A. Revell, H. Iacovides, and W. Wu, "Numerical prediction of local hot-spot phenomena in transformer windings," *Appl. Therm. Eng.*, vol. 36, no. 1, pp. 96–105, 2012.
[8] M. E. Rosillo, C. A. Herrera, and G. Jaramillo, "Advanced thermal modeling and experimental performance of oil distribution transformers," *IEEE Trans. Power Deliv.*, vol. 27, no. 4, pp. 1710–1717,

2012.
[9] F. Torriano, P. Picher, and M. Chaaban, “Numerical investigation of 3D flow and thermal effects in a disc-type transformer winding,” *Appl. Therm. Eng.*, vol. 40, pp. 121–131, 2012.
[10] M. A. Tsili, E. I. Amoiralis, A. G. Kladas, and A. T. Souflaris, “Power transformer thermal analysis by using an advanced coupled 3D heat transfer and fluid flow FEM model,” *Int. J. Therm. Sci.*, vol. 53, pp. 188–201, 2012.
[11] F. Torriano, H. Campelo, M. Quintela, P. Labbé, and P. Picher, “Numerical and experimental thermofluid investigation of different disc-type power transformer winding arrangements,” *Int. J. Heat Fluid Flow*, vol. 69, no. November 2017, pp. 62–72, 2018.
[12] R. Lecuna, F. Delgado, A. Ortiz, P. B. Castro, I. Fernandez, and C. J. Renedo, “Thermal-fluid characterization of alternative liquids of power transformers: A numerical approach,” *IEEE Trans. Dielectr. Electr. Insul.*, vol. 22, no. 5, pp. 2522–2529, 2015.
[13] I. Fernández *et al.*, “Thermal degradation assessment of Kraft paper in power transformers insulated with natural esters,” *Appl. Therm. Eng.*, vol. 104, 2016.
[14] T. W. Park and S. H. Han, “Numerical analysis of local hot-spot temperatures in transformer windings by using alternative dielectric fluids,” *Electr. Eng.*, vol. 97, no. 4, pp. 261–268, 2015.
[15] A. Santisteban, F. Delgado, A. Ortiz, I. Fernandez, C. J. Renedo, and F. Ortiz, “Numerical analysis of the hot-spot temperature of a power transformer with alternative dielectric liquids,” *IEEE Trans. Dielectr. Electr. Insul.*, vol. 24, no. 5, 2017.
[16] A. Santisteban, A. Piquero, F. Ortiz, F. Delgado, and A. Ortiz, “Thermal Modelling of a Power Transformer Disc Type Winding Immersed in Mineral and Ester-Based Oils Using Network Models and CFD,” *IEEE Access*, vol. 7, pp. 174651–174661, 2019.
[17] C. P. McShane, “Vegetable-oil-based dielectric Coolants,” *IEEE Ind. Appl. Mag.*, vol. 8, no. 3, pp. 34–41, 2002.
[18] L. Yang, B. Deng, R. Liao, C. Sun, and M. Zhu, “Influence of vegetable oil on the thermal aging rate of Kraft paper and its mechanism,” *Gaodianya Jishu/High Volt. Eng.*, vol. 38, no. 8, pp. 2059–2067, 2012.
[19] J. Carcedo, I. Fernández, A. Ortiz, F. Delgado, C. J. Renedo, and C. Pesquera, “Aging assessment of dielectric vegetable oils,” *IEEE Electr. Insul. Mag.*, vol. 31, no. 6, pp. 13–21, 2015.
[20] A. A. Abdelmalik, J. C. Fothergill, and S. J. Dodd, “Aging of Kraft paper insulation in natural ester dielectric fluid,” *Proc. IEEE Int. Conf. Solid Dielectr. ICSD*, pp. 541–544, 2013.
[21] R. Liao, S. Liang, C. Sun, L. Yang, and H. Sun, “A comparative study of thermal aging of transformer insulation paper impregnated in natural ester and in mineral oil,” *Eur. Trans. Electr. Power*, vol. 20, no. April 2009, p. n/a-n/a, 2009.
[22] G. R. Rodriguez, L. Garelli, M. Storti, D. Granata, M. Amadei, and M. Rossetti, “Numerical and experimental thermo-fluid dynamic analysis of a power transformer working in ONAN mode,” *Appl. Therm. Eng.*, vol. 112, pp. 1271–1280, 2017.
[23] Z. R. Radakovic and M. S. Sorgic, “Basics of detailed thermal-hydraulic model for thermal design of oil power transformers,” *IEEE Trans. Power Deliv.*, vol. 25, no. 2, pp. 790–802, 2010.